ACS APPLIED MATERIALS & INTERFACES

Research Article

www.acsami.org

Evaluating the Effects of Charged Oligopeptide Motifs Coupled with RGD on Osteogenic Differentiation of Mesenchymal Stem Cells

Feng-Yi Cao, Wei-Na Yin, Jin-Xuan Fan, Li Tao, Si-Yong Qin, Ren-Xi Zhuo, and Xian-Zheng Zhang*

Key Laboratory of Biomedical Polymers of Ministry of Education & Department of Chemistry, Wuhan University, Wuhan 430072, People's Republic of China

Supporting Information

ABSTRACT: Mesenchymal stem cells, due to their multilineage differentiation potential, have emerged as a promising cell candidate for cell-based therapy. In recent years, biomaterials were artificially synthesized to control the differentiation of mesenchymal stem cells. In this study, a series of charged or neutral oligopeptide motifs coupled with RGD were synthesized and used for surface modification using quartz substrates as model. Cell behaviors on the modified surfaces with different charged oligopeptide motifs were studied. It was found that these different charged oligopeptide motifs coupled with RGD were biocompatible for cell proliferation and adhesion. Moreover, it was demonstrated that the positively charged oligopeptide motif could inhibit osteogenic differentiation, while the negatively charged and neutral oligopeptide motifs could enhance osteogenic differentiation in the presence of RGD. This work may bring us enlightenment that different charged oligopeptide motifs coupled with RGD may be used for biomaterial surface modification for different stem cell-based therapies.

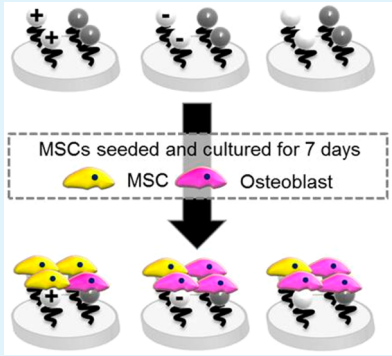

KEYWORDS: *charged oligopeptide, RGD, cBMHP1, stem cell, osteogenic differentiation*

1. INTRODUCTION

Mesenchymal stem cells (MSCs) are multilineage potential stem cells that can differentiate into a series of cells, such as adipocyte, chondrocyte, and osteoblast.[1] Because MSCs can be readily isolated from versatile tissues including brain, bone marrow, heart, and muscle[2,3] and expanded in vitro,[4] they have attracted great attention for stem cell-based therapy. In recent years, biomaterials were designed and synthesized artificially for in vivo and in vitro cell culture.[5−8] The biomaterials provide niches for cells to live in, while for anchorage-dependent stem cells such as MSCs, the biomaterial surface offers places for cells to locate on. It also was reported that their characteristics such as surface stress, geometry, charge, and growth factors have a great influence on cell behaviors.[9−13] Therefore, biomaterial surface modification is an effective method that can be used to control stem cell fate.

Arg-Gly-Asp (RGD) tripeptide motif, which was derived from extracellular matrices (ECM) proteins such as fibronectin, laminin, and collagen, was identified as one of the peptide sequences recognized by several cell membrane integrins.[14−16] To date, RGD has been extensively studied and applied in surface modification as it can enhance cell adhesion through integrin-mediated adhesion.[17−20] Moreover, cyclic RGD (cRGD), which had been verified to have approximately 2 orders of magnitude higher affinity for the $\alpha_v\beta_3$ integrin and may be more stable and have more biological advantages for in vivo applications, was demonstrated to induce osteogenic differentiation of MSCs by influencing cytoskeleton tension.[21,22]

Under physiological condition, molecules containing carboxyl and amino groups are charged compounds that may have an influence on cell behaviors through electrostatic interactions.[23−25] Chen and his group had reported that PAAc micropatterns could enhance adipogenic differentiation at the single-cell level and the differentiation extent had a relationship with the diameter of the pattern.[26] Yasuda and co-workers synthesized hydrogels with various charge densities, and it was found that they could enhance in vitro differentiation of chondrogenic ATDC5 cells.[27] However, the study of different charged compounds on mesenchymal stem cell osteogenic differentiation is still limited and remains to be explored.

In this work, different charged oligopeptide motifs coupled with RGD, c(RGD-K), c(RGD-D), and c(RGD-G), were synthesized to evaluate the effects of charge in the presence of RGD on osteogenic differentiation of mesenchymal stem cells (Scheme 1). A previous study by Ding's group synthesized a series of peptides with both cyclic RGD and linear charged or neutral oligopeptides, and made the first examination of the charge effect in the presence of cRGD on adhesion of NIH/3T3 fibroblast cells.[28] In this work, we combined RGD motif and charged or neutral oligopeptide motifs into one cycle to examine their effect on osteogenic differentiation of MSCs. To our knowledge, it was the first study of the effect of charge in the presence of RGD on osteogenic differentiation of mesenchmal stem cells. To further study their effects on osteogenic

Received: January 4, 2015
Accepted: March 6, 2015
Published: March 6, 2015

DOI: 10.1021/acsami.5b00064
ACS Appl. Mater. Interfaces 2015, 7, 6698−6705

Scheme 1. (A) Chemical Structures of the Synthesized Cyclic Peptides Containing Both Different Charged Oligopeptide Motifs and RGD; and (B) Schematic Representation of the Different Peptides Tethered to the Substrates and Their Effects on Osteogenic Differentiation of MSCs

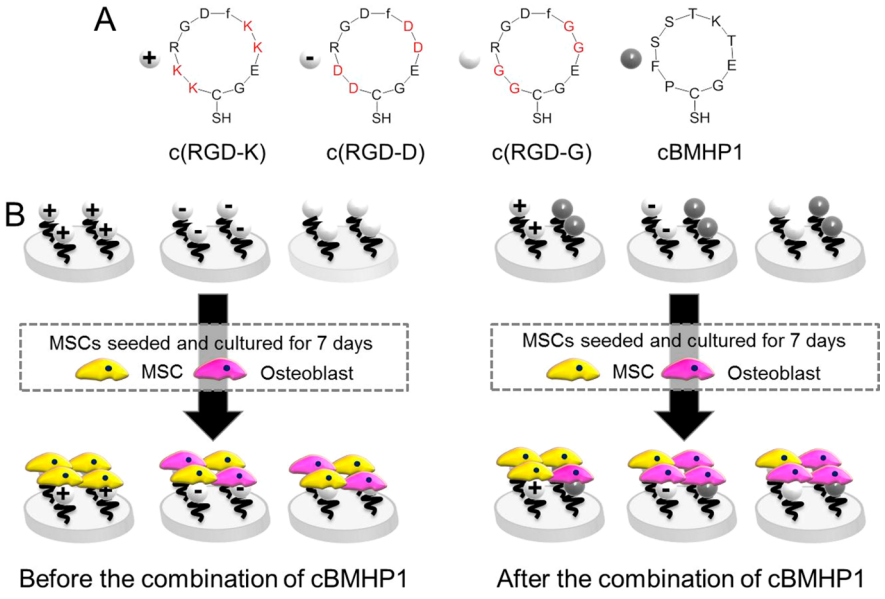

differentiation, a cyclic bone homing peptide (cBMHP1), which was confirmed in our previous study that it could enhance osteogenic differentiation of MSCs with or without the presence of osteogenic differentiation medium,[29] was introduced to evaluate whether they had a synergic effect with the different charged oligopeptide motifs or not.

2. EXPERIMENTAL SECTION

2.1. Synthesis and Characterization of the Peptide Linkers. The peptide linkers, c(RGD-K), c(RGD-D), c(RGD-G), and cBMHP1, were manually synthesized on the rink amine-AM resin (0.059 mmol/g) based on a standard Fmoc solid-phase method.[30] The resin and all of the Fmoc-protecting amino acids were purchased from GL Biochem Ltd. (China). Lysine (K), aspartic acid (D), and glycine (G) were used to construct charged motifs because under physiological condition, K is positively charged, D is negatively charged, and G is neutral. In addition, glutamic acid (E) was used for peptide cyclization, and cysteine (C) was used as a linker for conjugating to the modified surface. To verify the peptides were successfully synthesized, the molecular weights were confirmed by an electrospray ionization mass spectrometry (ESI−MS) system (Finnigan LCQadvantage).

2.2. Surface Modifications and Contact Angle Measurements. Surface modification was carried out on quartz substrates (15 mm × 1 mm, 15 mm × 3 mm). The quartz substrates were chosen as a model for surface modification. To tether the peptide linkers, primary surface modifications were carried out on quartz substrates to form maleimide terminated self-assembly monolayers as previously reported.[27] Briefly, the quartz substrates were cleaned in "piranha" solution (30% H_2O_2:98% H_2SO_4 = 3:7, v:v) to form hydroxyl self-assembly monolayers (OH-SAMs). The OH-SAMs then were incubated with 3-aminopropyltrimethoxysilane (APTMS) to form amidogen self-assembly monolayers (NH_2-SAMs). Third, the NH_2-SAMs were incubated with 0.02 M 3-maleimidopropionic acid to form maleimide self-assembly monolayers (MA-SAMs). The synthesized peptide (0.125 mg/mL) was conjugated to the modified substrates via Michael addition to form peptide self-assembly monolayers (Peptide-SAMs). To study the synergic effect of cBMHP1 with each charged oligopeptide motif coupled with RGD on stem cell differentiation, cBMHP1 was further conjugated, and the weight ratio of cBMHP1 and peptide containing both the charged oligopeptide motif and the RGD was 1:1. Noted here, after the combination of cBMHP1, the surfaces were marked with "+" following the relative peptide.

Static water contact angles on each surface were measured using the sessile drop method on a JC2000A optical contact angle meter (Powereach, China).

Table 1. ESI−MS Analysis of All of the Synthesized Peptides

peptide	M (calcd)	m/z (found)
c(RGD-K)	1275.7	638.74, 1277.11, 1278.20
c(RGD-D)	1223.4	1222.4, 1223.4
c(RGD-G)	991.4	922.83, 993.98
cBMHP1	1036.5	1037.6

2.3. Isolation and Culture of Bone Mesenchymal Stem Cells (MSCs). MSCs were harvested from 5-week-old male SD rats according to the method previously reported.[31] Sprague−Dawley (SD) rats were purchased from the Laboratory Animal Center of Zhongnan Hospital of Wuhan University (China), and all of the animal experiments were approved by the Animal Research Committee of Zhongnan Hospital of Wuhan University and conducted in accordance with the guidelines of the Experimental Animals Management Committee (Hubei Province, China). The medium (low glucose Dulbecco's modified Eagle's medium, 10% FBS, 1% penicillin-streptomycin) was changed every 3 days, and after cells reached 80−90% confluence, they were detached with trypsin-EDTA solution. All of the cells used in this Article were from passage 2−3. For each parallel group, the cells were from the same passage. For cell culture, the peptide modified substrates and blank quartz substrates were first sterilized under UV irradiation for 30 min, and then put into 24-well plates.

2.4. Cell Viability. Cell viability was measured using 3-(4,5-dimethylthiazol-2-yl)-2,5-diphenyltetrazolium bromide (MTT) assay. MSCs were seeded at a density of 3×10^4/well and incubated in 1 mL of maintenance medium for 7 days; the medium was changed every 3 days. Next, 100 μL of MTT (5 mg/mL) was added to each well and incubated for another 4 h. Subsequently, the medium was completely removed, and 1 mL of DMSO was added to dissolve formazan extraction. After being shaken for 5 min, 200 μL of the mixture from each well was removed to a 96-well plate, and the plate was read from a microplate reader (Bio-Rad, model 550, U.S.) at 570 nm. The relative cell viability was assessed choosing the OD value of cells on the blank quartz substrate as 100%.

DOI: 10.1021/acsami.5b00064
ACS Appl. Mater. Interfaces 2015, 7, 6698−6705

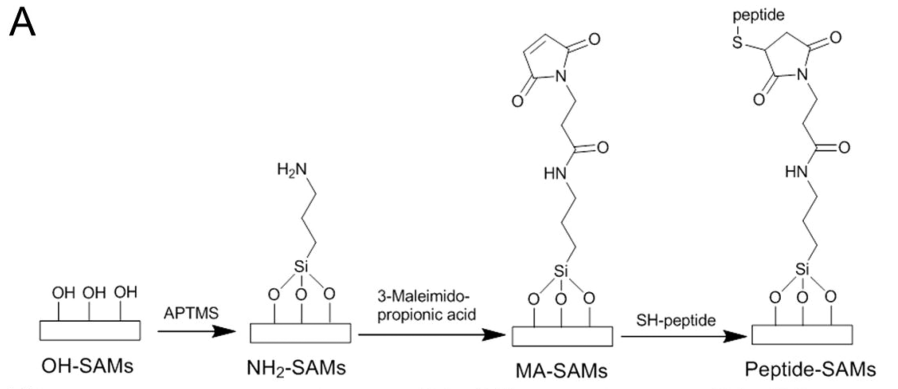

Peptide-SAMs	c(RGD-K)	c(RGD-D)	c(RGD-G)	c(RGD-K)+	c(RGD-D)+	c(RGD-G)+	cBMHP1
CA((θ)	51.6 ± 4.5	43.2 ± 3.5	45.4 ± 2.6	45.9 ± 3.4	48.7 ± 4.5	51.9 ± 3.0	50.8± 3.9

Figure 1. (A) Schematic procedure of the surface modifications on the quartz substrates via a layer-by-layer strategy. (B) Contact angles on each modified surface.

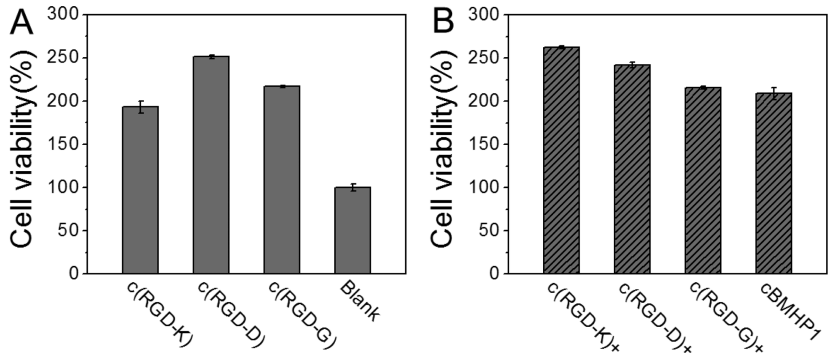

Figure 2. Cell viability on the different peptide modified and blank surfaces after cell culture for 7 days: (A) before the combination of cBMHP1, and (B) after the combination of cBMHP1, choosing cell viability on the blank surface as 100%.

2.5. Cell Adhesion. For the cell adhesion assay, cells were seeded at a density of 2×10^4/well and cultured for 3 h, then the medium was aspirated and cells were rinsed with PBS two times to remove the nonadherent cells. Subsequently, cells were fixed with 4% paraformaldehyde and the F-actin was stained using CF488A-Phalloidin (Biotium, U.S.), and the nuclei were stained with Hoechst 33258 (Lonza Corp., U.S.). Cells were observed on a confocal laser scanning microscope (CLSM) (C1-Si, Nikon, Japan), and the images were analyzed using Image-J software.

2.6. Osteogenic Differentiation. For the osteogenic differentiation assay, cells were seeded at a density of 3×10^4/well and cultured for another 7 days in maintenance medium, and osteogenesis markers were evaluated.

For Runx2 staining, cells were fixed and the F-actin was stained with CF488A-Phalloidin. The cells were first stained with primary rabbit antibody against rabbit Runx2 (Santa Cruz, U.S.) (1:100) for 1 h, followed by goat antirabbit IgG-Cy3 (Boster, China) (1:100) stained for 40 min. The immunofluorescence stain was observed on a confocal laser scanning microscope.

To evaluate the expression of alkaline phosphatase (ALP), cells were lysed with 0.2 mL of 1% Triton X-100. The total protein concentration then was measured using a BCA protein assay kit (Pierce, U.S.), and ALP activity was measured according to the ALP kits protocol (Nanjing Jiancheng Bioengineering Institute, China). The relative ALP activity was assessed choosing the ALP activity value of cells on the blank quartz substrate as 100%.

For Alizarin Red S staining, cells were fixed and stained with 1% Alizarin Red S (Sigma-Aldrich) solution (Tris-HCl buffer, pH = 8.3) for 30 min. The substrates were removed from the cell culture 24-well plate and rinsed in PBS buffer twice. Images were snapped after the substrates were dried out. For quantitative analysis, the Alizarin Red S stained on each substrate was dissolved in 0.2 mL of 10% cetylpyridinumchloride (Biosharp, China) in 10 mM sodiumphosphate. After being incubated in 37 °C for 30 min, 100 μL of the mixture from each well was removed to a 96-well plate, and the absorbance values were measured at 620 nm from a microplate reader.

3. RESULTS AND DISCUSSION

3.1. Formation of Different Peptide Modified Surfaces. The peptide linkers were manually synthesized on the basis of a standard Fmoc solid-phase method (Supporting Information Scheme S1), and the molecular weights of c(RGD-K), c(RGD-D), (cRGD-G), and cBMHP1 peptides were determined by ESI−MS (Supporting Information Figures S1−S4). The results of ESI−MS are shown in Table 1. The different peptide modified surfaces were prepared using a layer-by-layer strategy as previously reported (Figure 1A). The contact angles on the primary

DOI: 10.1021/acsami.5b00064
ACS Appl. Mater. Interfaces 2015, 7, 6698−6705

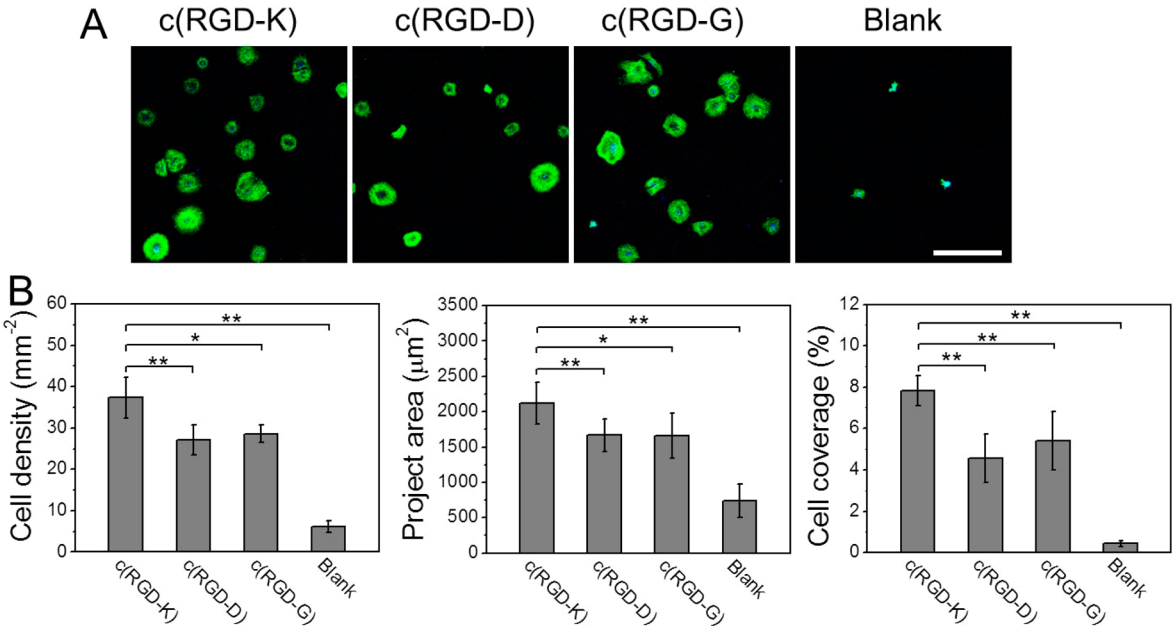

Figure 3. Cell adhesion on the different peptide modified and blank surfaces for 3 h before the combination of cBMHP1. (A) CLSM images of cells adhered: F-actin (green), nuclei (blue). The scale bar is 200 μm. (B) Statistical quantification of cell density, average cell project area, and cell coverage of cells adhered via software Image-J. Mean ± SD, *p < 0.05 and **p < 0.01.

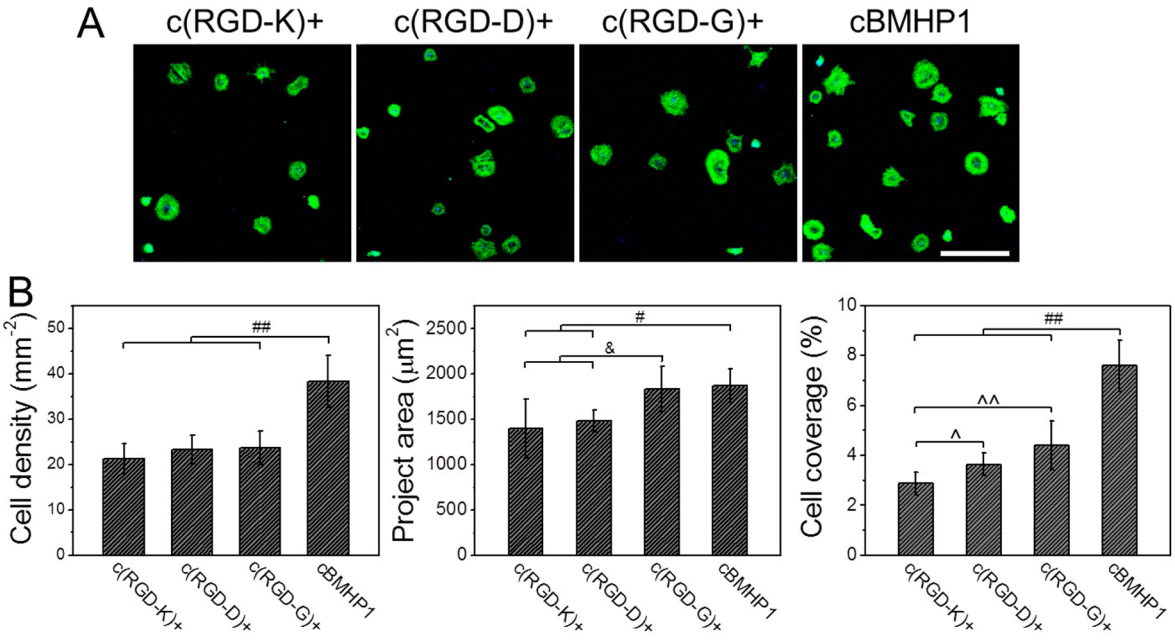

Figure 4. Cell adhesion on the different peptide modified and cBMHP1 surfaces for 3 h after the combination of cBMHP1. (A) CLSM images of cells adhered: F-actin (green), nuclei (blue). The scale bar is 200 μm. (B) Statistical quantification of cell density, average cell project area, and cell coverage of cells adhered via software Image-J. Mean ± SD, #p < 0.05 and ##p < 0.01; &p < 0.05; ∧p < 0.05 and ∧∧p < 0.01.

modified and peptides modified surfaces are listed in Figure 1B. The contact angle on the unmodified OH-SAMs was just 11.6° ± 1.5°. The formation of NH_2-SAMs increased the contact angle to 42.3° ± 2.1°. After the formation of MA-SAMs, the contact angle increased to 46.3° ± 3.7°. There was no obvious difference of the contact angles on the different peptide modified surfaces. Noted here, after the combination of cBMHP1, the surfaces were marked with "+" following the relative peptide.

3.2. Cell Viability on the Different Peptide Modified Surfaces. Cell biocompatibility is the basic requirement for biomaterials used for cell culture and tissue engineering. Cell viability was evaluated on the different peptide modified surfaces by MTT assay. As shown in Figure 2, after cell culture for 7 days, the numbers of living cells on the different peptide modified surfaces before and after the combination of cBMHP1 were 2−3 times that on the blank quartz surface, confirming that all of the different peptides modified surfaces were more biocompatible than the blank quartz surface. It also agreed with literature reports that RGD and BMHP1 peptides could promote cell proliferation.[32,33] These results confirmed that these different charged oligopeptide motifs coupled with RGD were biocompatible for surface modification.

DOI: 10.1021/acsami.5b00064
ACS Appl. Mater. Interfaces 2015, 7, 6698−6705

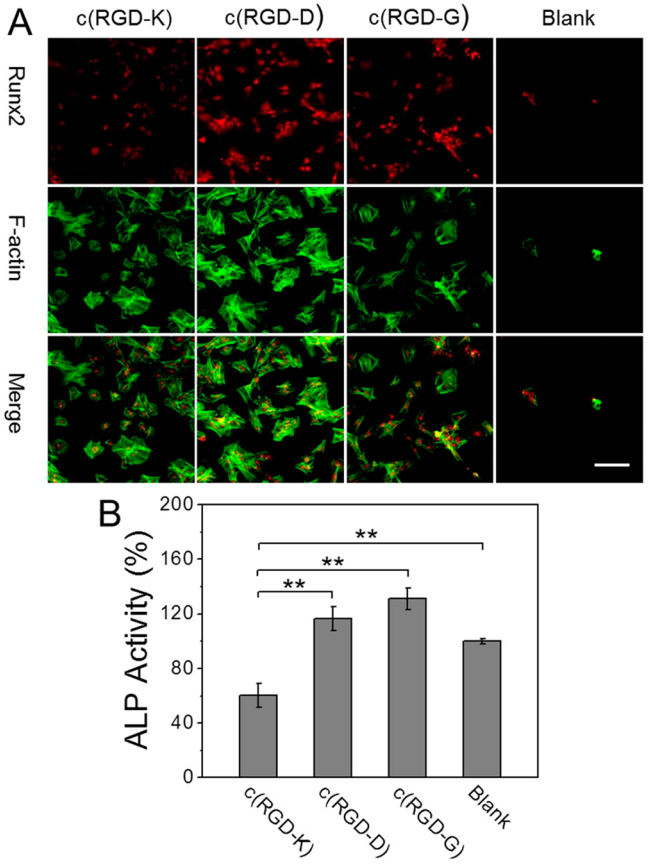

Figure 5. Runx2 and ALP evaluated on the different peptide modified and blank surfaces after 7-day culture before the combination of cBMHP1. (A) CLSM images of Runx2 staining: Runx2 (red), F-actin (green). The scale bar is 100 μm. (B) The relative ALP expression using blank as 100%. Mean ± SD, *p < 0.05 and **p < 0.01.

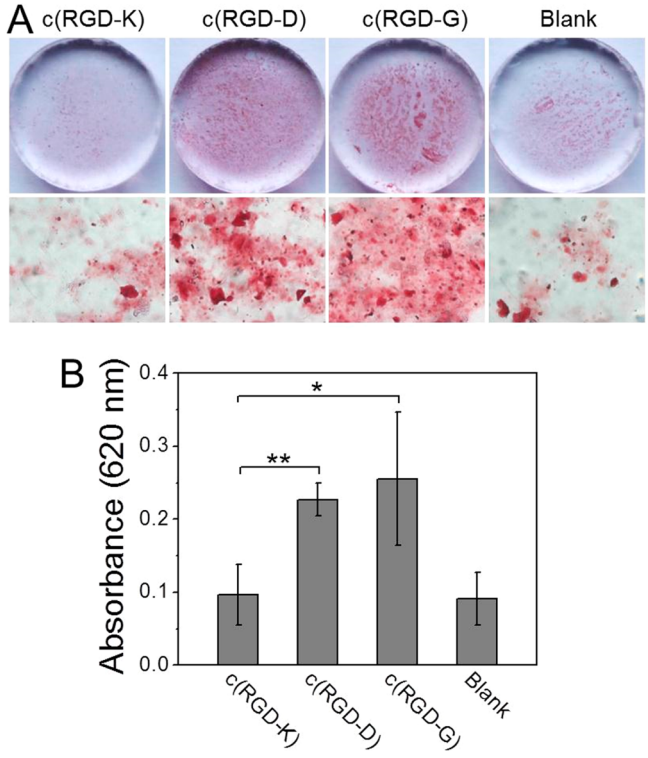

Figure 6. Calcium deposits evaluated on the different peptide modified and blank surfaces after 7-day culture before the combination of cBMHP1. (A) Alizarin Red S staining: the top shows macroscopic images, and the bottom shows low magnification inverted micrographs (200×). (B) Quantitative colorimetric results of Ca^{2+} expression. Mean ± SD, *p < 0.05 and **p < 0.01.

3.3. Cell Adhesion on the Different Peptide Modified Surfaces. To evaluate the effects of charge on cell adhesion, MSCs were seeded on the different peptide modified surfaces for 3 h. The CLSM images and image analysis by Image-J are shown in Figures 3 and 4. Before the combination of cBMHP1 (Figure 3), the cell density, average cell project area, and cell coverage on the c(RGD-K) modified surface were much larger than that on the c(RGD-D) and c(RGD-G) modified surfaces. Besides, cell adhesions on the c(RGD-D) and c(RGD-G) modified surfaces were similar. These findings were consistent with a previous report by Ding and his group that cells preferentially adhered to the positively charged surface as compared to the negatively charged or neutral surfaces.[28] This study also indicated that the positively charged oligopeptide motif could promote cell adhesion whether it was in the RGD cycle or not, while cells could hardly adhere on the blank surface because it was hydrophilic and without any conjugated biomolecules. These results confirmed that the c(RGD-K) containing a positively charged oligopeptide motif could enhance cell adhesion as compared to c(RGD-D) and c(RGD-G) containing negatively charged or neutral oligopeptide motifs, and all of the peptide modified surfaces were compatible for cell adhesion as compared to the blank surface.

After the combination of cBMHP1 (Figure 4), there was no obvious difference of cell density on the c(RGD-K)+, c(RGD-D)+, and c(RGD-G)+ modified surfaces, while cell density on the cBMHP1 modified surface was much larger. The average project area and cell coverage on the c(RGD-G)+ and cBMHP1 modified surfaces were larger than those on the c(RGD-K)+ and c(RGD-D)+ modified surfaces. It was also found that cell adhesions on the cBMHP1 and c(RGD-K) modified surfaces were similar. These agreed with previous reports that the degree of cell attachment of BMHP1 was much higher than that of linear RGD, and BMHP1 could bind to stem cells.[33,34] We could surmise that after the combination of cBMHP1, the effect of different charged oligopeptide motifs on cell adhesion was restrained. However, all of the peptide modified surfaces were compatible for cell adhesion.

3.4. Osteogenic Differentiation on the Different Peptide Modified Surfaces before the Combination of cBMHP1. Upon osteogenic differentiation, Runx2, ALP, and mineral deposition were confirmed as osteogenic markers.[35−37] Runx2 and ALP were early markers of osteogenesis. Mineral deposition was generated in the late stage of osteogenic differentiation, and calcium deposition could be detected by Alizarin Red S staining. After 7-day culture, as demonstrated in Figure 5, the expression of Runx2 (Figure 5A) on the c(RGD-K) modified surface was lower than that on the blank surface. Moreover, the expression of ALP on the c(RGD-K) modified surface was only about 60% of that on the blank surface (Figure 5B), while on the c(RGD-D) and c(RGD-G) modified surfaces, the expressions of Runx2 and ALP were several times higher than that on the blank surfaces. Besides, the expressions of Runx2 and ALP on the c(RGD-D) and c(RGD-G) modified surfaces were similar.

Calcium deposits stained by Alizarin Red S are shown in Figure 6A, and the quantitative results are shown in Figure 6B.

DOI: 10.1021/acsami.5b00064
ACS Appl. Mater. Interfaces 2015, 7, 6698−6705

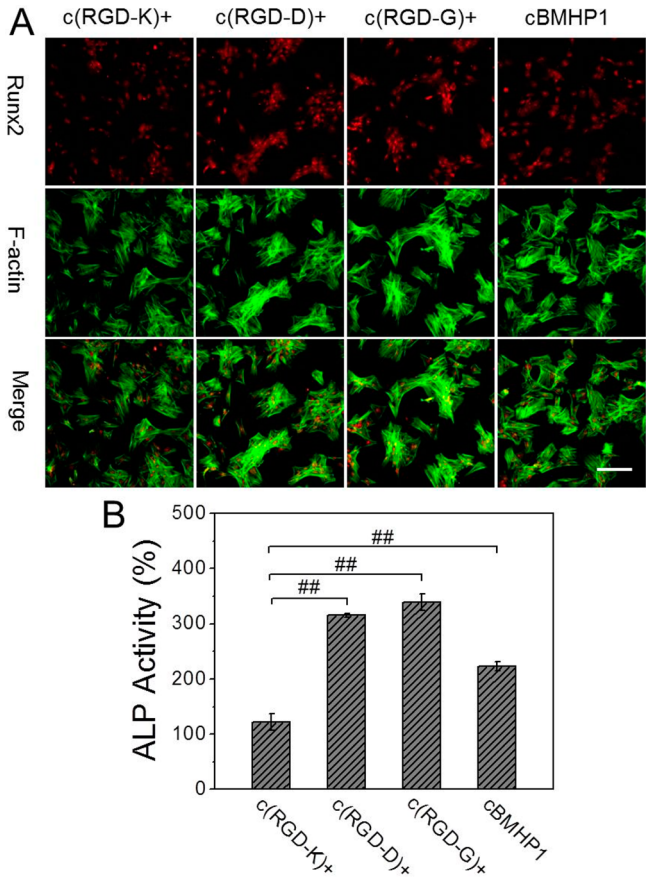

Figure 7. Runx2 and ALP evaluated on the different peptide modified surfaces after 7-day culture after the combination of cBMHP1. (A) CLSM images of Runx2 staining: Runx2 (red), F-actin (green). The scale bar is 100 μm. (B) The relative ALP expression using blank as 100%. Mean ± SD, ##p < 0.01.

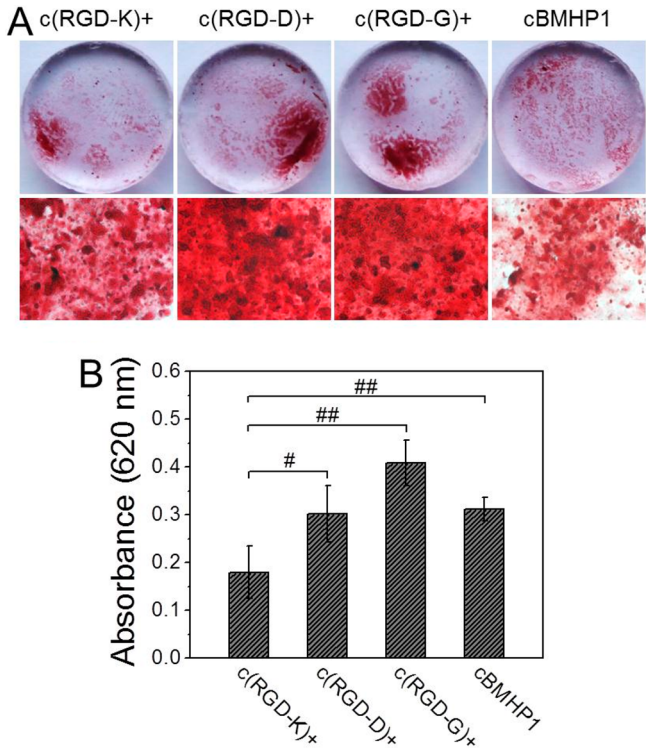

Figure 8. Calcium deposits evaluated on the different peptide modified surfaces after 7-day culture after the combination of cBMHP1. (A) Alizarin Red S staining: the top shows macroscopic images, and the bottom shows low magnification inverted micrographs (200×). (B) Quantitative colorimetric results of Ca^{2+} expression. Mean ± SD, #p < 0.05 and ##p < 0.01.

The intensity of calcium deposits and expression of Ca^{2+} on the c(RGD-K) modified surface were similar to those on the blank surface, while the intensity of calcium deposits and expressions of Ca^{2+} on the c(RGD-D) and c(RGD-G) modified surfaces were several times higher than those on the blank and c(RGD-K) modified surfaces. Also, the intensity of calcium deposits and expressions of Ca^{2+} on the c(RGD-D) and c(RGD-G) modified surfaces were similar. These results confirmed that the c(RGD-D) and c(RGD-G) containing negatively charged or neutral oligopeptide motifs could enhance osteogenic differentiation, while the c(RGD-K) containing a positively charged oligopeptide motif could inhibit osteogenic differentiation.

3.5. Osteogenic Differentiation on the Different Peptide Modified Surfaces after the Combination of cBMHP1. After the combination of cBMHP1, as shown in Figure 7, the expression of Runx2 (Figure 7A) on the c(RGD-K)+ modified surface was lower than that on the c(RGD-D)+ and c(RGD-G)+ modified surfaces, while the expression of Runx2 on the c(RGD-K)+ modified surface was slightly lower than that on the cBMHP1 modified surface. The expressions of ALP (Figure 7B) on the c(RGD-D)+ and c(RGD-G)+ modified surfaces were about 2−3 times that on the c(RGD-K)+ modified surface, while the expression of ALP on the c(RGD-K)+ modified surface was only about one-half of that on the cBMHP1 modified surface.

The intensity of calcium deposits (Figure 8A) and expression of Ca^{2+} (Figure 8B) on the c(RGD-K)+ modified surface were less than those on the cBMHP1 modified surface. Also, the expression of Ca^{2+} on the c(RGD-D)+ modified surface was less than that on the c(RGD-G)+ modified surface. In addition, calcium deposits on the cBMHP1 modified surface were uniform, while calcium deposits on c(RGD-D)+ and c(RGD-G)+ modified surfaces tended to aggregate and form a rich matrix with the highest intensity of red color, indicating that osteogenesis on the c(RGD-D)+ and c(RGD-G)+ modified surfaces reached a higher extent. These results confirmed that with the combination of osteogenic cBMHP1 peptide, although c(RGD-K)+ containing a positively charged oligopeptide motif could slightly enhance MSCs osteogenic differentiation, the function of cBMHP1 was inhibited, and the c(RGD-D)+ and c(RGD-G)+ containing negatively charged or neutral oligopeptide motifs could enhance the function of cBMHP1.

Previous reports confirmed that MSCs tended to differentiate toward osteogenic program when cultured on stiff substrates or cell adhesion ligands modified surfaces.[38,39] In this study, although c(RGD-K) containing a positively charged oligopeptide motif could promote cell adhesion, the trend toward osteogenic differentiation was smaller as compared to c(RGD-D) and (RGD-G) containing negatively charged or neutral oligopeptide motifs. Although cell adhesion on the cBMHP1 was much better, the trend toward osteogenic differentiation was medium. This was similar to the study by Ding and his group that, although a small RGD nanospacing induced a strong focal adhesion and distinct cytoskeleton, it had a small trend to osteogenic differentiation.[20] It was hypothesized that a better cell adhesion does not always accompany a better cell osteogenic differentiation. From this study, we could confirm that a

DOI: 10.1021/acsami.5b00064
ACS Appl. Mater. Interfaces 2015, 7, 6698−6705

positively charged oligopeptide motif could inhibit osteogenic differentiation, and negatively charged or neutral oligopeptide motifs could promote osteogenic differentiation in the presence of RGD.

4. CONCLUSION

In summary, a series of peptides containing both different charged oligopeptide motifs and RGD were synthesized, and their effects on MSC behaviors were evaluated. It was found that all of the peptide modified surfaces were biocompatible for cell proliferation and adhesion. Moreover, osteogenic differentiation studies demonstrated that c(RGD-K) containing a positively charged oligopeptide motif could inhibit osteogenic differentiation, while c(RGD-D) and c(RGD-G) containing negatively charged or neutral oligopeptide motifs could enhance osteogenic differentiation whether with the combination of osteogenic peptide or not. Our study has shown that these different charged oligopeptide motifs coupled with RGD may be used for surface modification on two-dimensional or three-dimensional biomaterials to control the differentiation of MSCs for stem cell-based therapy.

■ ASSOCIATED CONTENT

Supporting Information

Scheme S1, synthesis procedure of the cyclic peptides, choosing c(RGD-K) as an example. Figures S1−S4, ESI−MS of the four cyclic peptides: c(RGD-K), c(RGD-D), c(RGD-G), and cBMHP1. This material is available free of charge via the Internet at http://pubs.acs.org.

■ AUTHOR INFORMATION

Corresponding Author

*Tel./fax: 86-27-68754509. E-mail: xz-zhang@whu.edu.cn.

Notes

The authors declare no competing financial interest.

■ ACKNOWLEDGMENTS

This work was supported by the financial support from the National Natural Science Foundation of China (51125014 and 51233003), the Ministry of Science and Technology of China (2011CB606202), and the Natural Science Foundation of Hubei Province of China (2013CFA003).

■ REFERENCES

(1) Pittenger, M. F.; Mackay, A. M.; Beck, S. C.; Jaiswal, R. K.; Douglas, R.; Mosca, J. D.; Moorman, M. A.; Simonetti, D. W.; Craig, S.; Marshak, D. R. Multilineage Potential of Adult Human Mesenchymal Stem Cells. *Science* **1999**, *284*, 143−147.

(2) Jiang, Y. H.; Jahagirdar, B. N.; Reinhardt, R. L. Pluripotency of Mesenchymal Stem Cells Derived from Adult Marrow. *Nature* **2002**, *418*, 41−49.

(3) Momin, E. N.; Mohyeldin, A.; Zaidi, H. A.; Vela, G.; Quiñones-Hinojosa, A. Mesenchymal Stem Cells: New Approaches for the Treatment of Neurological Diseases. Curr. *Stem Cell Res. Ther.* **2010**, *5*, 326−344.

(4) Da Silva Meirelles, L.; Chagastelles, P. C.; Nardi, N. B. Mesenchymal Stem Cells Reside in Virtually All Post-Natal Organs and Tissues. *J. Cell Sci.* **2006**, *119*, 2204−2213.

(5) Lee, I. C.; Liu, Y. C.; Tsai, H. A.; Shen, C. N.; Chang, Y. C. Promoting the Selection and Maintenance of Fetal Liver Stem/Progenitor Cell Colonies by Layer-by-Layer Polypeptide Tethered Supported Lipid Bilayer. *ACS Appl. Mater. Interfaces* **2014**, *6*, 20654−20663.

(6) Tatavarty, R.; Ding, H.; Lu, G. J.; Taylor, R. J.; Bi, X. H. Synergistic Acceleration in the Osteogenesis of Human Mesenchymal Stem Cells by Graphene Oxide-Calcium Phosphate Nanocomposites. *Chem. Commun.* **2014**, *50*, 8484−8487.

(7) Lutolf, M. P.; Gilbert, P. M.; Blau, H. M. Designing Materials to Direct Stem-Cell Fate. *Nature* **2009**, *462*, 433−441.

(8) Higuchi, A.; Ling, Q. D.; Hsu, S. T.; Umezawa, A. Biomimetic Cell Culture Proteins as Extracellular Matrices for Stem Cell Differentiation. *Chem. Rev.* **2012**, *112*, 4507−4540.

(9) Guilak, F.; Cohen, D. M.; Estes, B. T.; Gimble, J. M.; Liedtke, W.; Chen, C. S. Control of Stem Cell Fate by Physical Interactions with the Extracellular Matrix. *Cell Stem Cell* **2009**, *5*, 17−26.

(10) Ayala, R.; Zhang, C.; Yang, D.; Hwang, Y. S.; Aung, A.; Shroff, S. S.; Arce, F. T.; Lal, R.; Arya, G.; Varghese, S. Engineering the Cell-Material Interface for Controlling Stem Cell Adhesion, Migration, and Differentiation. *Biomaterials* **2011**, *32*, 3700−3711.

(11) Shi, X. T.; Li, L.; Ostrovidov, S.; Shu, Y. W.; Khademhosseini, A.; Wu, H. K. Stretchable and Micropatterned Membrane for Osteogenic Differentation of Stem Cells. *ACS Appl. Mater. Interfaces* **2014**, *6*, 11915−11923.

(12) Wang, Y.; Yao, S. L.; Meng, Q. Y.; Yu, X. L.; Wang, X. M.; Cui, F. Z. Gene Expression Profiling and Mechanism Study of Neural Stem Cells Response to Surface Chemistry. *Reg. Bio.* **2014**, *1*, 37−47.

(13) Yao, X.; Peng, R.; Ding, J. D. Cell-Material Interactions Revealed Via Material Techniques of Surface Patterning. *Adv. Mater.* **2013**, *25*, 5257−5286.

(14) Ruoslahti, E. RGD and Other Recognition Sequences for Integrins. *Annu. Rev. Cell Dev. Biol.* **1996**, *12*, 697−715.

(15) Chastain, S. R.; Kundu, A. K.; Dhar, S.; Calvert, J. W.; Putnam, A. J. Adhesion of Mesenchymal Stem Cells to Polymer Scaffolds Occurs via Distinct ECM Ligands and Controls their Osteogenic Differentiation. *J. Biomed. Mater. Res., Part A* **2006**, *78*, 73−85.

(16) Iwamoto, M. E.; Iwamoto, M.; Nakashima, K.; Mukudai, Y.; Boettiger, D.; Pacifici, M.; Kurisu, K.; Suzuki, F. Involvement of $\alpha_5\beta_1$ Integrin in Matrix Interactions and Proliferation of Chondrocytes. *J. Bone Miner. Res.* **1997**, *12*, 1124−1131.

(17) Hersel, U.; Dahmen, C.; Kessler, H. RGD Modified Polymers: Biomaterials for Stimulated Cell Adhesion and Beyond. *Biomaterials* **2003**, *24*, 4385−4415.

(18) Neffa, J. A.; Tresco, P. A.; Caldwell, K. D. Surface Modification for Controlled Studies of Cell-Ligand Interactions. *Biomaterials* **1999**, *20*, 2377−2393.

(19) McNichols, C.; Wilkins, J.; Kubota, A.; Shiu, Y. T.; Aouadi, S. M.; Kohli, P. Investigating Surface Topology and Cyclic-RGD Peptide Functionalization on Vascular Endothelialization. *J. Biomed. Mater. Res., Part A* **2014**, *102*, 532−539.

(20) Wang, X.; Yan, C.; Ye, K.; He, Y.; Li, Z. H.; Ding, J. D. Effect of RGD Nanospacing on Differentiation of Stem Cells. *Biomaterials* **2013**, *34*, 2865−2874.

(21) Kilian, K. A.; Mrksich, M. Directing Stem Cell Fate by Controlling the Affinity and Density of Ligand-Receptor Interactions at the Biomaterials Interface. *Angew. Chem., Int. Ed.* **2012**, *51*, 4891−4895.

(22) Hsiong, S. X.; Boontheekul, T.; Huebsch, N.; Mooney, D. J. Cyclic Arginine-Glycine-Aspartate Peptides Enhance Three-Dimensional Stem Cell Osteogenic Differentiation. *Tissue Eng., Part A* **2009**, *15*, 263−272.

(23) Calabrese, R.; Kaplan, D. L. Silk Ionomers for Encapsulation and Differentiation of Human MSCs. *Biomaterials* **2012**, *33*, 7375−7385.

(24) Lu, H. X.; Guo, L. K.; Kawazoe, N.; Tateishi, T.; Chen, G. P. Effects of Poly(L-lysine), Poly(acrylic acid) and Poly(ethylene glycol) on the Adhesion, Proliferation and Chondrogenic Differentiation of Human Mesenchymal Stem Cells. *J. Biomater. Sci., Polym. Ed.* **2009**, *20*, 577−589.

(25) Schröder, K.; Finke, B.; Ohl, A.; Lüthen, F.; Bergemann, C.; Nebe, B.; Rychly, J.; Walschus, U.; Schlosser, M.; Liefeith, K.; Neumann, H. G.; Weltmann, K. D. Capability of Differently Charged

DOI: 10.1021/acsami.5b00064
ACS Appl. Mater. Interfaces 2015, 7, 6698−6705

Plasma Polymer Coating for Control of Tissue Interactions with Titanium Surfaces. *J. Adhes. Sci. Technol.* **2010**, *24*, 1191−1205.
(26) Song, W.; Wang, X. L.; Lu, H. X.; Kawazoe, N.; Chen, G. P. Exploring Adipogenic Differentiation of a Single Stem Cell on Poly(acrylic acid) and Polystyrene Micropatterns. *Soft Matter* **2012**, *8*, 8429−8437.
(27) Kwon, H. J.; Yasuda, K.; Ohmiya, Y.; Honma, K. I.; Chen, Y. M.; Gong, J. P. In Vitro Differentiation of Chondrogenic ATDC5 Cells Is Enhanced by Culturing on Synthetic Hydrogels with Various Charge Densities. *Acta Biomater.* **2010**, *6*, 494−501.
(28) Lai, Y. X.; Xie, C.; Zhang, Z.; Lu, W. Y.; Ding, J. D. Design and Synthesis of a Potent Peptide Containing both Specific and Non-specific Cell-Adhesion Motifs. *Biomaterials* **2010**, *31*, 4809−4817.
(29) Cao, F. Y.; Yin, W. N.; Fan, J. X.; Zhuo, R. X.; Zhang, X. Z. A Novel Function of BMHP1 and cBMHP1 Peptides to Induce the Osteogenic Differentiation of Mesenchymal Stem Cells. *Biomater. Sci.* **2015**, *3*, 345−351.
(30) Qin, S. Y.; Jiang, H. F.; Liu, X. J.; Pei, Y.; Cheng, H.; Sun, Y. X.; Zhang, X. Z. High Length-Diameter Ratio Nanotubes Self-Assembled from a Facial Cyclopeptide. *Soft Matter* **2014**, *10*, 947−951.
(31) Soleimani, M.; Nadri, S. A Protocol for Isolation and Culture of Mesenchymal Stem Cells from Mouse Bone Marrow. *Nat. Protoc.* **2009**, *4*, 102−106.
(32) Wohlrab, S.; Müller, S.; Schmidt, A.; Neubauer, S.; Kessler, H.; Leal-Egaña, A.; Scheibel, T. Cell Adhesion and Proliferation on RGD-Modified Recombinant Spider Silk Proteins. *Biomaterials* **2012**, *28*, 6650−6659.
(33) Gelain, F.; Bottai, D.; Vescovi, A.; Zhang, S. G. Designer Self-Assembling Peptide Nanofiber Scaffolds for Adult Mouse Neural Stem Cell 3-Dimensional Cultures. *PLoS One* **2006**, *1*, e119.
(34) Nowakowski, G. S.; Dooner, M. S.; Valinski, H. M.; Mihaliak, A. M.; Quesenberry, P. J.; Becker, P. S. A Specific Heptapeptide from a Phage Display Peptide Library Homes to Bone Marrow and Binds to Primitive Hematopoietic Stem Cells. *Stem Cells* **2004**, *22*, 1030−1038.
(35) Ducy, P.; Zhang, R.; Geoffroy, V.; Ridall, A. L.; Karsenty, G. Osf2/Cbfa1: A Transcriptional Activator of Osteoblast Differentiation. *Cell* **1997**, *89*, 747−754.
(36) He, T. C.; Luo, X. J.; Chen, J.; Song, W. X.; Tang, N.; Luo, J. Y.; Deng, Z. L.; Sharff, K. A.; He, G.; Bi, Y.; He, B. C.; Bennett, E.; Huang, J. Y.; Kang, Q.; Jiang, W.; Su, Y. X.; Zhu, G. H.; Yin, H.; He, Y.; Wang, Y.; Souris, J. S.; Chen, L.; Zuo, G. W.; Montag, A. G.; Reid, R. R.; Haydon, R. C.; Luu, H. H. Osteogenic BMPs Promote Tumor Growth of Human Osteosarcomas That Harbor Differentiation Defects. *Lab. Invest.* **2008**, *88*, 1264−1277.
(37) Sun, H. L.; Feng, K.; Hu, J.; Soker, S.; Atala, A.; Ma, P. X. Osteogenic Differentiation of Human Amniotic Fluid-Derived Stem Cells Induced by Bone Morphogenetic Protein-7 and Enhanced by Nanofibrous Scaffolds. *Biomaterials* **2010**, *31*, 1133−1139.
(38) Engler, A. J.; Sen, S.; Sweeney, H. L.; Discher, D. E. Matrix Elasticity Directs Stem Cell Lineage Specification. *Cell* **2006**, *126*, 677−689.
(39) Martino, M. M.; Mochizuki, M.; Rothenfluh, D. A.; Rempel, S. A.; Hubbell, J. A.; Barker, T. H. Controlling Integrin Specificity and Stem Cell Differentiation in 2D and 3D Environments through Regulation of Fibronectin Domain Stability. *Biomaterials* **2009**, *30*, 1089−1097.

DOI: 10.1021/acsami.5b00064
ACS Appl. Mater. Interfaces 2015, 7, 6698−6705